Separation Science and Technology
Publication details, including instructions for authors and subscription information:
http://www.informaworld.com/smpp/title~content=t713708471

Modeling the Influence of Temperature on Resistance of Concentration Layer and Transmembrane Flux in Reverse Osmosis Systems

Sergei P. Agashichev[a]
[a] Research Center-ADWEA, Abu Dhabi, United Arab Emirates

To cite this Article Agashichev, Sergei P.(2004) 'Modeling the Influence of Temperature on Resistance of Concentration Layer and Transmembrane Flux in Reverse Osmosis Systems', Separation Science and Technology, 39: 14, 3215 — 3236
To link to this Article: DOI: 10.1081/SS-200033170
URL: http://dx.doi.org/10.1081/SS-200033170

SEPARATION SCIENCE AND TECHNOLOGY
Vol. 39, No. 14, pp. 3215–3236, 2004

Modeling the Influence of Temperature on Resistance of Concentration Layer and Transmembrane Flux in Reverse Osmosis Systems

Sergei P. Agashichev[*]

Research Center-ADWEA, Abu Dhabi, United Arab Emirates

ABSTRACT

Model permits analyzing the influence of temperature on resistance of concentration layer and transmembrane flux. Proposed model is based on the following assumptions: (1) membrane morphology doesn't depend on temperature; (2) membrane rejection, and other transport characteristics of membrane are invariant with coordinate; (3) specific water permeability of membrane was based on exponential dependence of viscosity vs. temperature; (4) dependence of membrane rejection on temperature is assumed to be linear. Dependence of normalized permeability upon temperature is strongly influenced by the CP degree (and surface concentration), namely, (A) at low CP degree the growth

---

[*] Correspondence: Sergei P. Agashichev, Research Center-ADWEA, P.O. Box 54111, Abu Dhabi, United Arab Emirates; E-mail: agashichev@netscape.net.

DOI: 10.1081/SS-200033170 0149-6395 (Print); 1520-5754 (Online)
www.dekker.com

of temperature causes growth of normalized permeability, while at (B) high values of CP degree the system is characterized by opposite behavior: the normalized permeability goes down with growth of temperature. The model allows analyzing the influence of temperature and degree of membrane rejection on concentration resistance and transmembrane flux. Calculated data are attached. The presented solution can be segmented and built into algorithm for calculation of longitudinal profile of CP degree and for optimization of regime parameters against temperature.

Key Words: Reverse osmosis; Modeling; Concentration polarization; Influence of temperature.

1. INTRODUCTION

Membrane separation is accompanied by unavoidable phenomenon referred to as the concentration polarization (CP). This phenomenon is quantified by the degree of concentration polarization that is equal to the ratio of difference between bulk and surface concentration to the bulk concentration. The CP phenomenon is dependent upon different physical factors and process variables. Many existing models ignore temperature-dependence of characteristics and assume the process behavior to be isothermal or temperature-independent. Some of them are based on simplifying assumptions implying temperature dependence only for diffusivity and viscosity coefficients, while the influence of temperature on resistance of concentration layer remains outside the scope of analysis.

2. FORMULATION OF THE PROBLEM

The influence of temperature is essential for the systems characterized by high permeate recovery, elevated feed temperature and high salinity of feed water. It is compulsory when seasonal variation of inlet temperature takes place in a wide range, these aspects are essential within the context of implementation of the RO technology in the Gulf Area.

The development of the new generation of integrated systems, namely triple hybrid including power generation, MSF and RO desalination (where the cooling water from the MSF heat rejection section is used as a feed for RO), is becoming an attractive technological alternative. Analysis of published data[1–5] outlines the following advantages of these systems: (1) ability to diversify range of the power- to water ratio; (2) possibility to use seasonal surplus of idle power; and (3) decrease specific energy consumption. Data published in[6] state that using the waste heat provides a saving of 15%. It is worth mentioning that the practical implementation of the integrated systems is hampered by lack of the methodology for modeling of temperature dependent behavior. Logical inconsistency between physical aspects and the assumptions, underlying the mathematical models, is inherited in many available software for calculation of concentration polarization.

Modeling of transport characteristics is considered in Refs.[7–9] Hydraulic membrane permeability, osmotic pressure, degree of concentration polarization, permeate recovery, specific energy consumption, etc., are strongly influenced by operating temperature. The influence of temperature on the permeate recovery and energy consumption is analyzed in Ref.[10] Results submitted in studies,[11] contain the influence of temperature on cumulative water output. Evaluation of RO pilot systems conducted in Abu Dhabi[12] demonstrated different functional behavior of membrane permeability vs. temperature at the 1st and 2nd RO stages. The 1st RO stage (45000 ppm) was characterized by a decrease of the normalized permeability with growth of feed water temperature, while the 2nd RO stage (500 ppm) was characterized by opposite behavior, the growth of temperature causes the growth of normalized permeability. (The permeability value recalculated at standard conditions, at $t = 20$ is referred to as normalized membrane permeability). The study[11] gave a set of experimental profiles for cumulative water output vs. temperature. Having been converted to normalized values, those profiles demonstrated a decrease of normalized permeability with growth of temperature as well.

Within the context of outlined problem, the proposed manuscript focuses on modeling of the influence of temperature on resistance and transmembrane flux. It is based on the following expression.

$$V(t,c) = \frac{\Delta P}{r_{mem}(t) + r_{CP\text{-}layer}(t,c) + r_{gel}(t,c)} \tag{1}$$

Where the transmembrane flux, V(t, c), is proportional to the driving force and inversely proportional to overall resistance that, in turn, depends on temperature and concentration. The nominator represents an overall driving force. The overall resistance (see denominator of Eq. (1) can be considered as sum of individual constituents namely: (1) temperature-dependent membrane resistance; (2) temperature- and concentration dependent resistance of CP layer, (3) temperature- and concentration dependent resistance of gel layer.

Resistance of the CP layer implies the contributions from the osmotic pressure.

3. UNDERLYING PREMISES AND ASSUMPTIONS OF THE MODEL

A symmetric plate-and-frame configuration of membrane system was considered in the study. An elementary parallelepiped was selected as a control volume. The fluid is assumed to be incompressible, continuous and isothermal with uniform density field under steady-state conditions All of characteristics are assumed to be position independent. Resistance of the gel layer assumed to be zero throughout the analysis. This term is outside the scope of the study, see Eq. (1). Further treatment is based on the following premises and simplifying assumptions.

3.1. Membrane Morphology (and Coefficient of Membrane Rejection)

Membrane is assumed to be a porous matrix with non-uniform capillary systems. Morphology of membrane is assumed to be temperature- and position-independent. Snow et al.,[9] give a set of profiles describing influence of temperature on degree of membrane rejection. In some cases the non-linearity can be ignored. Membrane rejection, $R_M(T)$, and other transport characteristics of membranes are assumed to be position- independent and linear with respect to temperature. The growth of temperature increases salt passage thus decreases the degree of membrane rejection. Temperature dependence of membrane rejection is expressed as:

$$R_{M(TRUE)}(T) = A_M T + B_M \tag{2}$$

Where $A_M = -4.4 \cdot 10^{-4}$, $B_M = 1.127$. Values of A_M and B_M in Eq. (2) are determined relying upon experimental data. They are fit to the data presented by *Snow et al.* in Ref.[9]

3.2. Concentration

Variation of concentration within the boundary layers is assumed in the model. It varies from C_1 in the bulk, to C_{1M} at the membrane surface, (see Fig. 1). It is caused by unbalanced transport between the bulk and membrane surface. This phenomenon is referred to as the concentration polarization

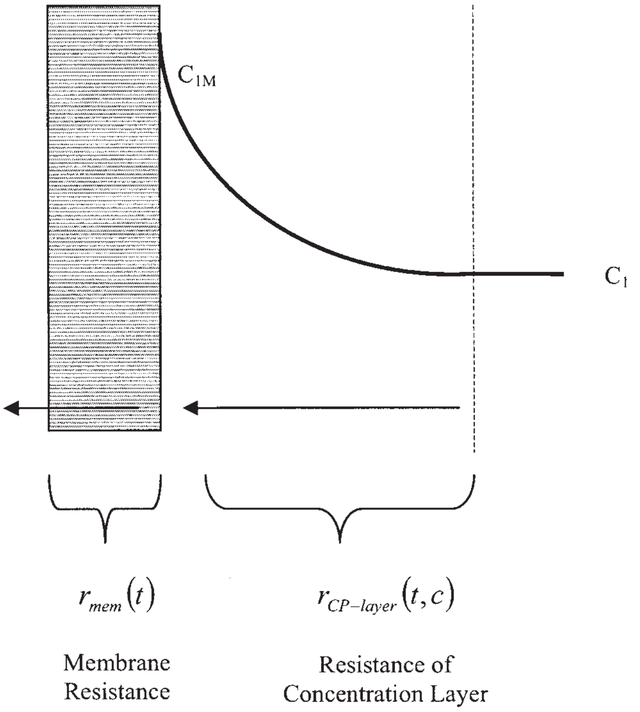

Figure 1. Concentration profile.

(CP), For quantification of the phenomenon, the degree of concentration polarization, α, is used.

$$\alpha = \frac{(C_{1M} - C_1)}{C_1} \tag{3}$$

The CP degree, in turn, is strongly influenced by the degree of membrane rejection and permeability. (Modeling of the influence of the degree of membrane rejection, R_M, on the CP degree is outside the scope of the study).

Assuming nonlinearity of concentration profile, membrane rejection can be expressed in terms of intrinsic (or true), $R_{M(TRUE)}$, and observed (or apparent), $R_{M(OBSERVED)}$, degree of membrane rejection.

$$R_{M(TRUE)} = \frac{(C_{1M} - C_2)}{C_{1M}} \tag{4}$$

$$R_{M(OBSERVED)} = \frac{(C_1 - C_2)}{C_1} \tag{5}$$

3.3. Physical Properties of Solution

Viscosity: Dependence of viscosity upon temperature, $\mu(T)$, is approximated by the Guzman-Andrade equation.[13]

$$\mu(T) = a\exp\left[\frac{b}{T}\right] \tag{6}$$

Osmotic pressure against temperature was approximated by linear function.

$$\pi(c, T) = icRT \tag{7}$$

Osmotic pressure under the surface concentration and in permeate, C_{1M} and C_2 respectively, can be expressed in terms of degree of CP and degree of membrane rejection. Surface value of osmotic pressure, $\pi(c_{1M})$ can be written as:

$$\pi(c_{1M}) = iC_1(1+\alpha)RT \tag{8}$$

Osmotic pressure of permeate in terms of true degree of rejection:

$$\pi(c_2) = iC_1(1+\alpha)(1-R_{M(TRUE)})RT \tag{9}$$

Osmotic pressure of permeate in terms of apparent degree of rejection:

$$\pi(c_2) = iC_1(1-R_{M(OBSERVED)})RT \tag{10}$$

4. MODELING

The section focuses on modeling of behavior of the following characteristics upon temperature- and concentration: (1) resistance of membrane matrix; (2) resistance of CP layer and (3) transmembrane flux.

4.1. Hydraulic Permeability and Resistance of Membrane Matrix

Hydraulic resistance of membrane, $r_{mem}(t)$, (see the first term in denominator in Eq. (1), is assumed to be concentration-independent and reciprocal to specific permeability of membrane, $A_{mem}(t)$. It gives.

$$r_{mem}(t) = A_{mem}^{-1}(t) \tag{11}$$

Where, $A_{mem}(t)$, temperature-dependent specific permeability of membrane. The dependence of $A_{mem}(t)$ upon temperature, in turn, is assumed to be based on exponential function for viscosity, $\mu(t)$.

$$A_{mem}(t) = A_{t0}\frac{\mu_{t0}}{\mu(t)} \tag{12}$$

Combining Eqs. (11), (12) and (6) we get

$$r_{mem}(t) = \frac{a}{A_{mem-t0}\mu_{t0}}\exp\left(\frac{b}{T}\right) \tag{13}$$

Where a & b are parameters from the Guzman- Andrade equation,[11] μ_{t0} and A_{mem-t0} are viscosity and specific permeability of membrane at the reference temperature. In the case study the specific permeability of membrane is assumed to be $A_{mem-t0} = 5.5 \cdot 10^{-7}\,\mathrm{m}^3/[\mathrm{m}^2\text{-s-bar}]$.

4.2. Hydraulic Resistance of the CP-Layer

In this study the CP layer is represented as a hydraulic resistance to transverse flux along with the resistance of membrane matrix itself. (See the second term in denominator of Eq. (1). Resistance of the CP layer depends on surface concentration and has to be expressed as a function of surface concentration. Using conventional relation, the transmembrane flux can be expressed in terms of the net driving force, (where the net driving force is the difference between operating pressure and osmotic pressure difference):

$$V(t, c) = A_{mem}(t)[\Delta P - \Delta\pi_{1M-2}(t, c)] \tag{14}$$

Combining Eqs. (14), (11) and (1), we get a relation between hydraulic resistance of CP layer, $r_{CP\text{-}layer}(t, c)$; transport characteristics of membrane, $A_{mem}(t)$; operating pressure difference and osmotic pressure. It can be written as follows:

$$r_{CP\text{-}layer}(t, c) = \frac{\Delta\pi_{1M-2}(t, c)}{A_{mem}(t)\,[\Delta P - \Delta\pi_{1M-2}(t, c)]} \tag{15}$$

Where

$$\begin{aligned}\Delta\pi_{1M-2} &= \pi(c_{1M}) - \pi(c_2) \\ &= i\lfloor(1+\alpha) - (1 - R_{M(OBSERVED)})\rfloor C_1RT \qquad (16)\end{aligned}$$

Combining Eqs. (13), (15) and (16) we get the function for hydraulic resistance of CP layer in terms of transport characteristics of membrane and process variables.

$$r_{CP\text{-}layer}(t,c) = \frac{a}{A_{mem(t0)}\mu_{t0}}\frac{i(R_{M(OBSERVED)}+\alpha)C_1RT}{[\Delta P - i(R_{M(OBSERVED)}+\alpha)C_1RT]}\exp\left(\frac{b}{T}\right) \qquad (17)$$

It can be rewritten in terms of $R_{M(TRUE)}$ as follows

$$r_{CP\text{-}layer}(t,c) = \frac{a}{A_{mem(t0)}\mu_{t0}}\frac{iR_{M(TRUE)}(\alpha+1)C_1RT}{[\Delta P - iR_{M(TRUE)}(\alpha+1)C_1RT]}\exp\left(\frac{b}{T}\right) \qquad (18)$$

Set of projections based on Eqs. (13) and (17) is shown in Fig. 2.

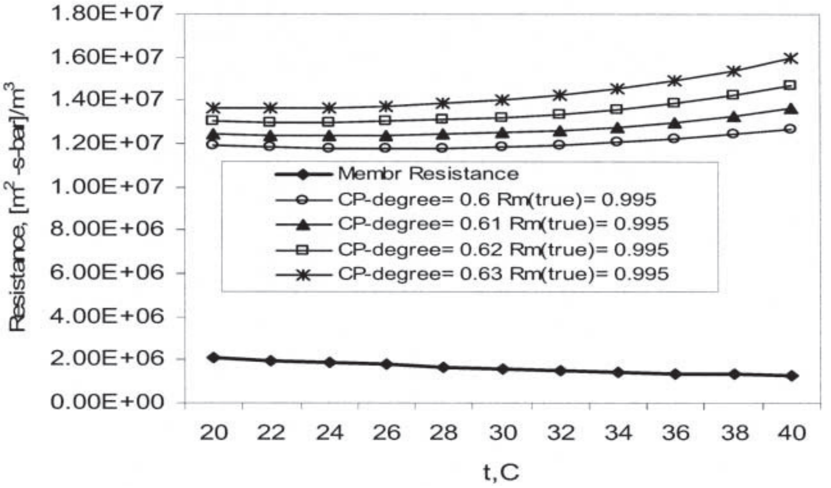

Figure 2. Influence of temperature on resistance of membrane (bottom curve) and diffusion layer (set of the top curves). Input data: $r_{mem(t=20)} = 1.82\text{E}+06$ [m^2-s-bar]/m^3, $A_{(t=20)} = 5.50\text{E}-07$ m^3/[m^2-s-bar], $\Delta P = 70$ bar, $C_1 = 45000$ ppm ($\sim$769 mol/m^3).

4.3. Transmembrane Flux

Calculation of transmembrane flux at operating temperature is based on Eq. (1) where the denominator represents the resistance of membrane and CP layer, see Eqs. (13) and (17) respectively. Set of calculated curves of specific permeability at operating temperature is shown in Fig. 3.

Behavior of the profiles shown in Fig.3 depends on the degree of CP and degree of membrane rejection. For the analysis of behavior to be done, the following extremal points should be determined: (1) point of minimum of CP resistance vs. temperature; and (2) upper limit of the CP degree.

4.4. Minimum of the CP resistance vs. Temperature (The First Derivative of the CP Resistance with Respect to Temperature)

The analysis of the CP resistance, (See Eqs. 18 and 17), is based on the first derivative with respect to temperature.

$$\frac{dr_{CP\text{-}layer}}{dT} = \frac{a}{A_{t0}\mu_{t0}} \frac{[b(1-k_2/T)+k_2]}{T^2(1-k_2/T)^2} \exp\left(\frac{b}{T}\right) \tag{19}$$

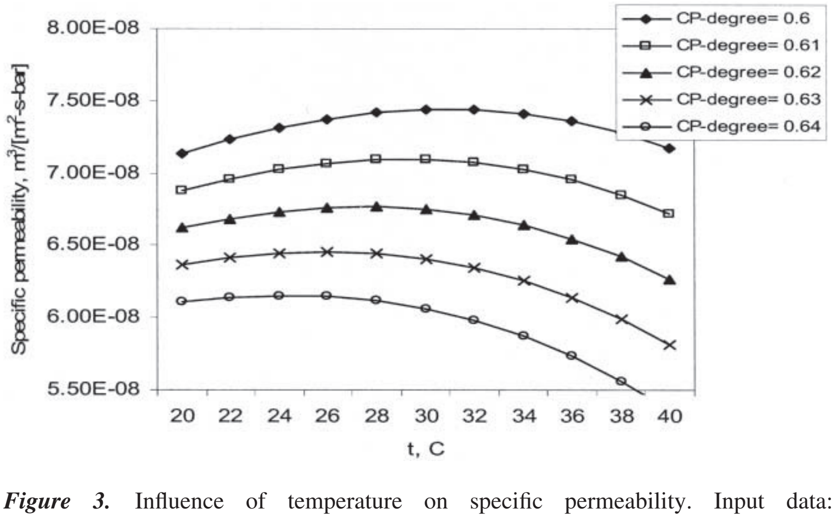

Figure 3. Influence of temperature on specific permeability. Input data: $r_{mem(t=20)} = 1.82\text{E}+06$ [m^2-s-bar]/m^3, $A_{(t=20)} = 5.50\text{E}-07$ m^3/[m^2-s-bar], $\Delta P = 70$ bar, $C_1 = 45000$ ppm ($\sim$769 mol/m^3).

Where

$$k_2 = \frac{\Delta P}{iC_1R(R_M + \alpha)} \tag{20}$$

In terms of $R_{M(TRUE)}$, it gives

$$k_2 = \frac{\Delta P}{iC_1RR_{M(TRUE)}(\alpha + 1)} \tag{21}$$

Behavior of the first derivative is influenced by membrane rejection and the CP degree, α, that is determined, in tern, by the degree of membrane rejection, R_M, as well. Modeling the functional interrelation between α and R_M is outside the scope of the study. In proposed analysis they are considered to be independent. A set of calculated projections at different values of CP degree is given in Fig. 4

Analysis of the first derivative gives location of the stationary points. The first derivative (Eq. (19) is equal to zero, $dr_{CP}/dT = 0$, at the point where the

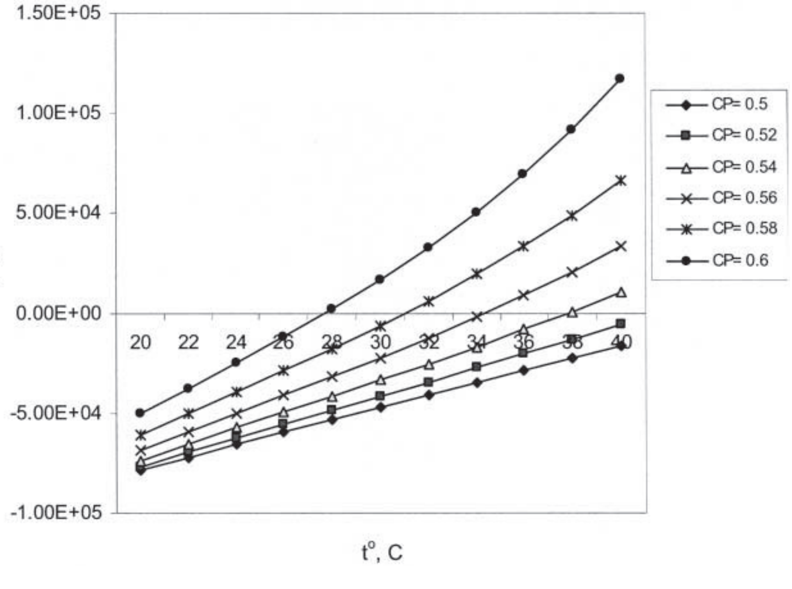

Figure 4. The first derivative of CP resistance with respect to operating temperature at various CP degree. Input data: R_M(true) = 0.99, $A_{(t=20)} = 5.50E{-}07\ m^3/[m^2\text{-s-bar}]$, $\Delta P = 70$ bar, $C_1 = 45000$ ppm ($\sim 769\ mol/m^3$).

inversion of functional behavior of the CP resistance against temperature takes place, (this point can be referred to as a critical point). Below the critical point, the growth of temperature decreases the CP resistance while above the point, the growth of temperature is accompanied by increase of the CP resistance. Being solved for temperature at the $dr_{CP}/dT = 0$, Eq. (19) gives the value of temperature where the inversion of behavior takes place. (It can be referred to as the critical value of temperature).

$$T_{crit}(\alpha, R_M) = \frac{k_2(\alpha, R_M)b}{k_2(\alpha, R_M) + b} \tag{22}$$

Where k_1 and k_2 are given by Eqs. (20) and (21), respectively.

The value of the critical temperature depends on the degree of membrane rejection, R_M, and is influenced by operating conditions such as the CP degree, α. Projections calculated at different values of the membrane rejection are given in Fig. 5. The curves indicate maximum attainable value of temperature above that the growth of temperature will increase the value of CP resistance. It is essential to consider in design in order to avoid undesirable growth of CP resistance.

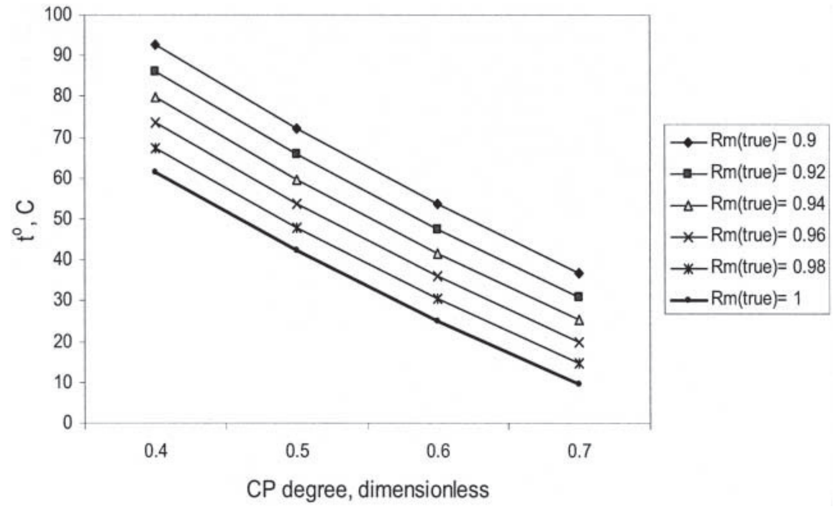

Figure 5. Critical temperature vs. CP degree at different values of membrane rejection Input data: $A_{(t=20)} = 5.50E-07\ m^3/[m^2\text{-s-bar}]$, $\Delta P = 70\ bar$, $C_1 = 45000\ ppm$ ($\sim 769\ mol/m^3$).

4.5. Upper Limit of CP-degree (Influence of Temperature and Membrane Rejection on the Upper Limit of CP-degree)

The growth of the surface concentration, C_{1M}, is limited by the surface osmotic pressure at the state of equilibrium that depends, in turn, on operating temperature and pressure. At the state of equilibrium (when the net driving force equals zero) the operating pressure difference is equal to osmotic pressure, $\Delta P = \Delta\pi_{1M-2}$.

$$\Delta P = i[C_{1M} - C_2]RT \tag{23}$$

The case expressed by Eq. (23) takes place at the maximum degree of CP. Denoting the CP degree at the state of equilibrium as $\alpha_{\max}(t)$ and combining Eqs. (23), (8) and (10) we get.

$$\Delta P = iC_1\lfloor(1 + \alpha_{\max}(t)) - (1 - R_{M(OBSERVED)})\rfloor RT \tag{24}$$

Being solved for $\alpha_{\max}(t)$, Eq. (24) gives

$$\alpha_{\max}(t) = \frac{\Delta P}{iC_1RT} - R_{M(OBSERVED)} \tag{25}$$

In terms of intrinsic (or true) degree of membrane rejection, the upper limit of CP degree (Eq. (25) can be rewritten as

$$\alpha_{\max}(t) = \frac{\Delta P}{R_{M(TRUE)}\,(iC_1RT)} - 1 \tag{26}$$

A growth of the degree of membrane rejection, R_M, decreases the upper limit of CP-degree. Fig. 6 gives a set of calculated projections in dimensionless form based on Eq. (26). A growth of the degree of membrane rejection increases a temperature dependence of the upper limit. (See a growth of the slope in Fig. 6). Calculated values of the upper limit based on Eq. (26) are given in Appendix A.

5. ANALYSIS OF THE SUBMODEL (INFLUENCE OF TEMPERATURE, DEGREE OF CONCENTRATION POLARIZATION AND DEGREE OF MEMBRANE REJECTION ON RESISTANCE OF THE CP LAYER)

The resistance of the CP layer (See Eq. 17) is influenced by the following process variables and membrane characteristics: temperature, concentration, operating pressure difference, the CP degree, membrane rejection, R_M, and specific permeability, $A_{mem}(t)$.

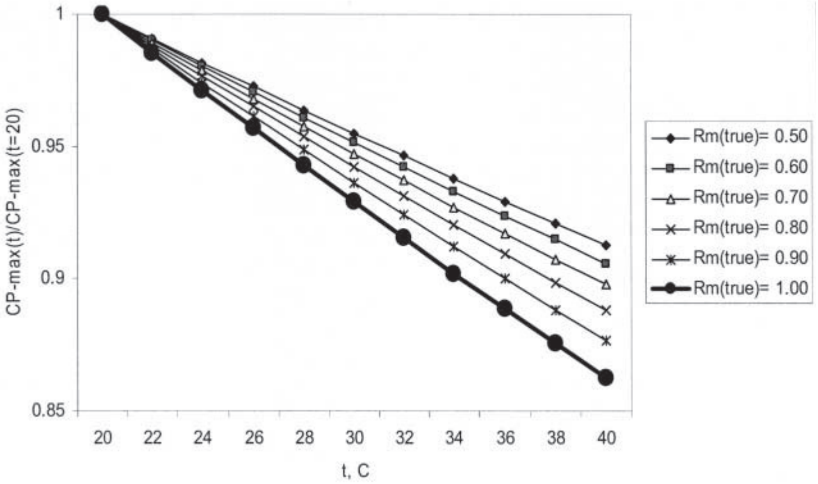

Figure 6. Upper limit of CP degree. Input data: $A_{(t=20)} = 5.50E-07\, m^3/[m^2\text{-s-bar}]$, $\Delta P = 70$ bar, $C_1 = 45000$ ppm ($\sim 769\, mol/m^3$).

5.1. Influence of Temperature on Resistance of the CP layer

A set of calculated projections of resistance of the CP layer, $r_{CP\text{-}layer}(t, c)$, vs. temperature (at different level of CP degree) is plotted in Fig. 7.

As shown in Fig. 7, the functional behavior is influenced by the level of CP degree and the surface concentration, namely at the low level of CP degree the growth of temperature decreases the CP resistance. A growth of the surface concentration can inverse the functional behavior, namely after the critical value of CP degree, the growth of temperature increases the resistance of CP-layer. Any individual value of the CP degree can be characterized by the temperature that corresponds to minimum value of the CP resistance. Profile describing the influence of temperature on the CP resistance at the arbitrary value of CP degree is shown in Fig. 8. (The profile is extracted from a set of calculated curves from Fig. 7).

5.1.1. Influence of Temperature on the Resistance of CP Layer at the High Level of CP Degree

Processes characterized by high and low values of the CP degree (therefore surface concentration) reveal different behavior with respect to temperature. In particular, the processes with a **high level of the CP degree** are

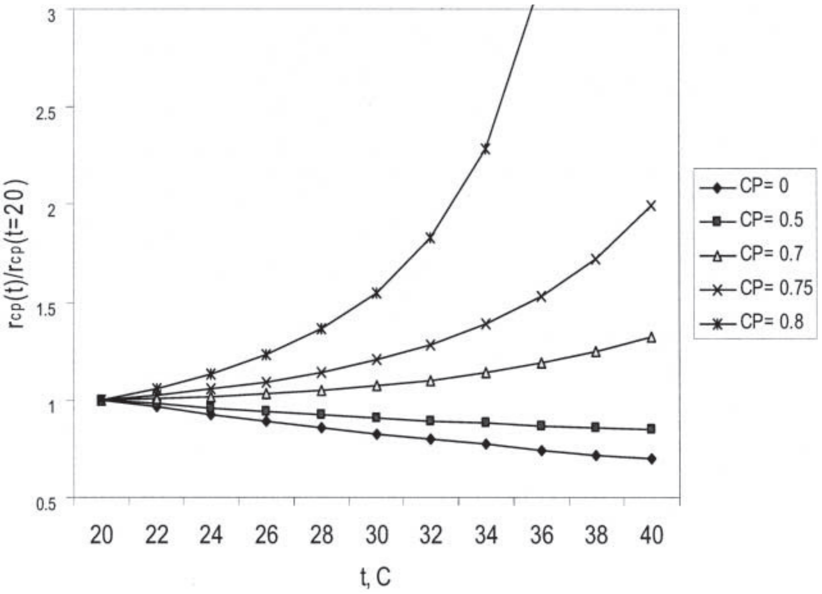

Figure 7. CP resistance vs. temperature at different CP degree Input data: R_M(true) = 0.97, $A_{(t=20)} = 5.50E-07\,m^3/[m^2\text{-s-bar}]$, $\Delta P = 70$ bar, $C_1 = 45000$ ppm (~769 mol/m^3).

controlled by a growth of the diffusion resistance, (see term in parenthesis in denominator of Eq. 17). A growth of the temperature, in this case, causes an increase of the resistance. A set of calculated projections for resistance of the CP layer, $r_{CP\text{-}layer}(t, c)$, vs. temperature is shown in Fig. 9. A similar behavior is typical for membranes on the 1st stage of RO systems.

5.1.2. Influence of Temperature on the Resistance of CP Layer at the Low Level of CP Degree

A process accompanied by low values of the CP degree is controlled by growth of hydraulic permeability of membranes, (see $A_{mem}(t)$ in denominator of Eq. (17)). A growth of temperature in this case is accompanied by the decrease of viscosity that, in turn, decreases the resistance. A similar behavior is typical for membranes with high permeability and moderate degree of rejection. A set of calculated projections for resistance of CP layer, $r_{CP\text{-}layer}(t, c)$, vs. temperature (for membrane with low degree of rejection) is shown in Fig. 10.

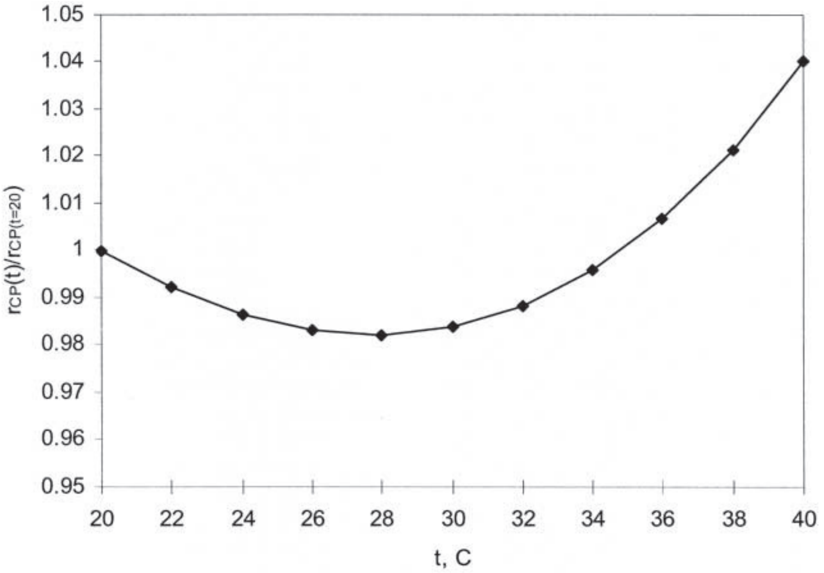

Figure 8. CP resistance vs. temperature. Input data: $R_M(\text{true}) = 0.99$, CP degree $= 0.6$, $A_{(t=20)} = 5.50\text{E}{-}07\,\text{m}^3/[\text{m}^2\text{-s-bar}]$, $\Delta P = 70\,\text{bar}$, $C_1 = 45000\,\text{ppm}$ ($\sim 769\,\text{mol/m}^3$).

Set of projections in dimensionless form vs. temperature at the various degree of membrane rejection. (The function is represented in dimensionless form as the ratio of resistance at operating temperature to resistance at reference temperature being equal to 20°C).

5.2. Influence of Temperature on Resistance of the CP layer at Different Degree of Membrane Rejection

Behavior of the CP resistance vs. temperature is dependent upon the degree of membrane rejection. Membranes characterized by high and low degree of rejection reveal different behavior with respect to operating temperature. In particular, growth of temperature for membranes with high degree of rejection causes non-linear increase of resistance, $r_{CP\text{-}layer}(t, c)$. (See top curves in Fig. 11). Membranes of this type are accompanied by a high level of the CP degree and, in turn, high surface concentration of the dissolved component. Similar behavior is typical for membranes on the 1st stage of RO systems. Growth of temperature for membranes with low

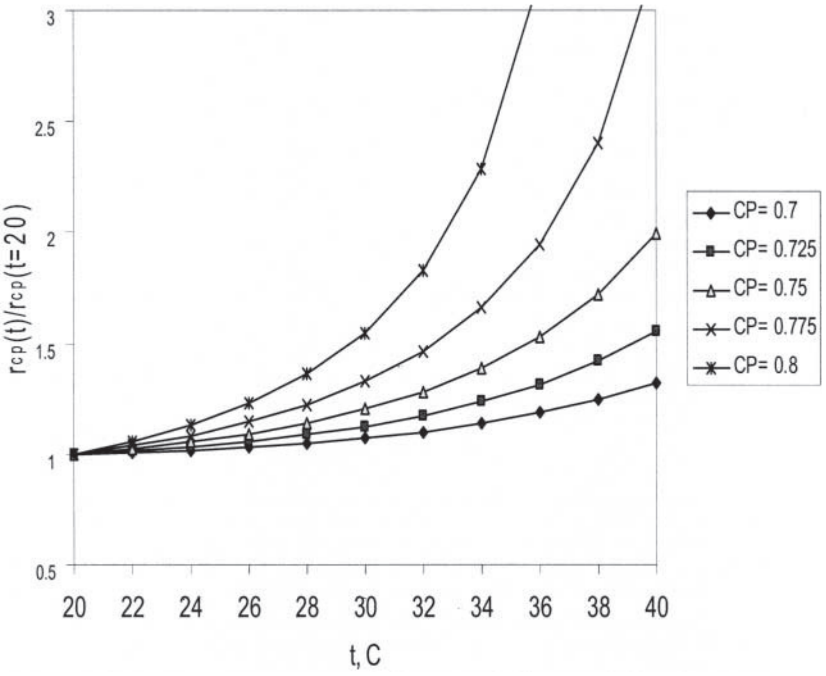

Figure 9. The CP resistance vs. temperature for the case of high level of CP degree. (CP degree ranges from 0.7 to 0.8). Input data: $R_M(\text{true}) = 0.97$, $A_{(t=20)} = 5.50E-07\ m^3/[m^2\text{-s-bar}]$, $\Delta P = 70\ \text{bar}$, $C_1 = 45000\ \text{ppm}$ ($\sim 769\ \text{mol}/m^3$)

degree of rejection causes decrease of resistance, $r_{CP\text{-}layer}(t, c)$. (See bottom curves in Fig. 11). This type of membrane is accompanied by low level of the CP degree and, in turn, low surface concentration of dissolved component. Behavior of resistance in this case is controlled by the influence of temperature on viscosity and, in turn, on hydraulic permeability of membrane itself, $A_{mem}(t)$. Similar behavior is typical for membranes on the 2nd stage of RO systems.

A model permits analyzing the influence of temperature on resistance of concentration layer and trans-membrane flux. A simplified sub-algorithm includes equations for calculation of the following characteristics: (1) membrane resistance, $r_{mem}(t)$, (2) resistance of the CP layer $r_{CP\text{-layer}}(t, c)$; and (3) transmembrane flux, V(t, c). See equations: Eq. (13); Eq. (18) and Eq. (1) respectively. For the longitudinal distribution of CP degree, the proposed submmodel can be consolidated with the equations describing longitudinal transport of component.

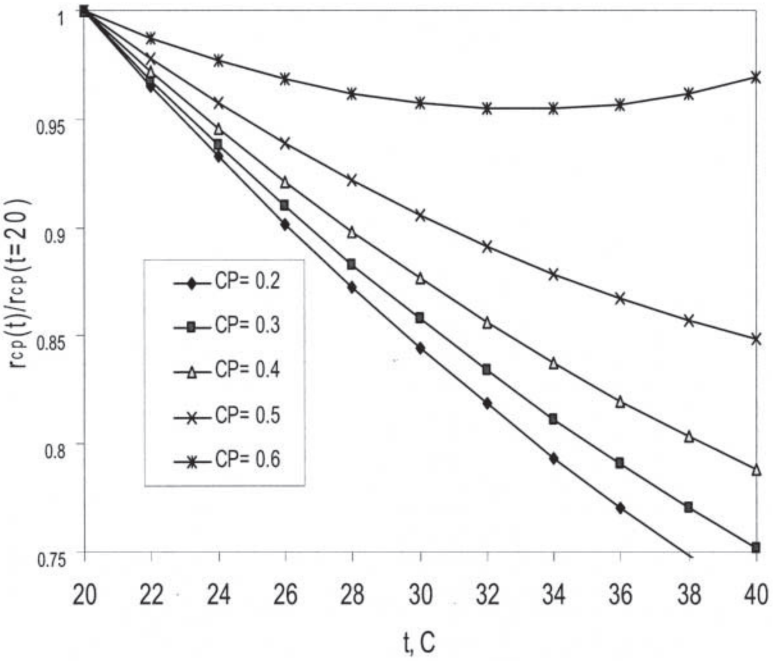

Figure 10. The CP resistance vs. temperature in the cases of low level of CP degree. (CP degree ranges from 0 to 0.5). Input data: R_M(true) $= 0.97$, $A_{(t=20)} = 5.50E-07\,m^3/[m^2\text{-s-bar}]$, $\Delta P = 70$ bar, $C_1 = 45000$ ppm ($\sim 769\,mol/m^3$), $a = 4.07 \cdot 10^{-7}$ PaS, $b = 2312$.

6. COMPARISON WITH EXPERIMENTAL AND PUBLISHED RESULTS

The calculated values of membrane permeability at operating temperature (based on Eq. 1) were converted to its normalized values and compared with experimental data. The following sources of data were used for comparison: (A) results published by Al-Bahri, Hanbury and Hodgkiess,[11]; (B) data received from existing RO plant (Al-Silla, UAE) and (C) data gathered during the pilot test of RO systems (Al-Tawelah, UAE).[12]

(A) The results given in study[11] show the influence of temperature on cumulative water output. It yielded a set of experimental profiles for cumulative water output vs. temperature. Having been converted to normalized values, those profiles demonstrate decrease of normalized permeability with growth of temperature (See Fig. 12).

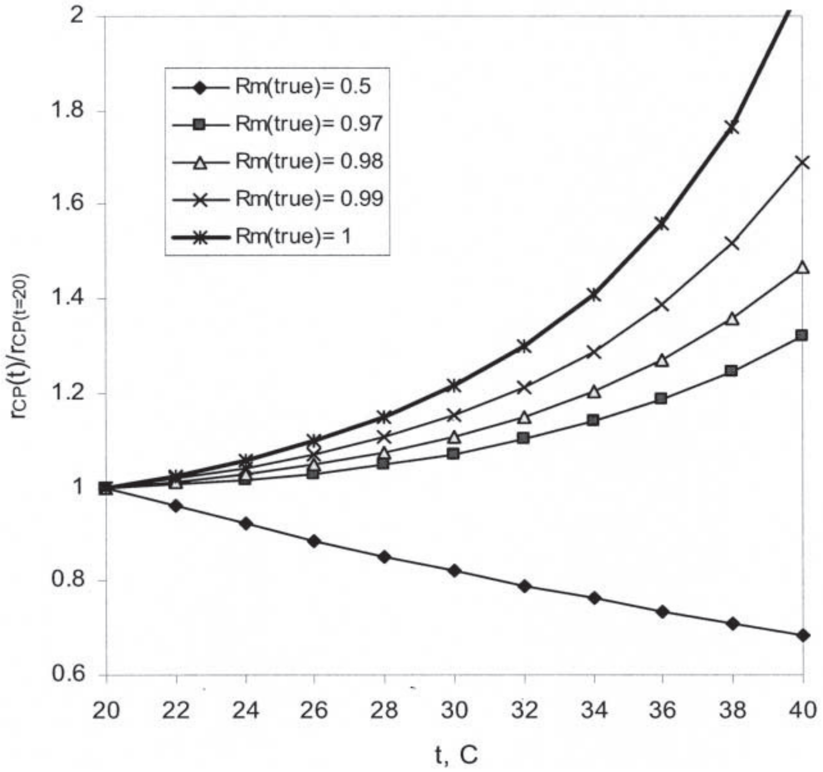

Figure 11. CP resistance vs. temperature at different degree of membrane rejection (True membrane rejection, M_R(true), ranges from 0.5 to 1) Input data: CP degree $= 0.7$, $A_{(t=20)} = 5.50E-07\,m^3/[m^2\text{-s-bar}]$, $\Delta P = 70$ bar, $C_1 = 45000$ ppm ($\sim 769\,mol/m^3$).

(B) The data on seasonal variation of membrane permeability, received from Al-Silla RO plant (UAE), revealed a decrease of normalized permeability against temperature (See Fig. 12).

(C) The pilot study conducted in Abu Dhabi,[12] demonstrated different functional behavior of membrane permeability vs. temperature at the 1st and 2nd RO stages. The 1st RO stage (~45000 ppm) was characterized by a decrease of the normalized permeability with growth of feed water temperature, while the 2nd RO stage (~500 ppm) revealed the opposite behavior, the growth of temperature causes the growth of normalized permeability. (The permeability value recalculated at referred conditions, t = 20, is referred to as normalized membrane permeability).

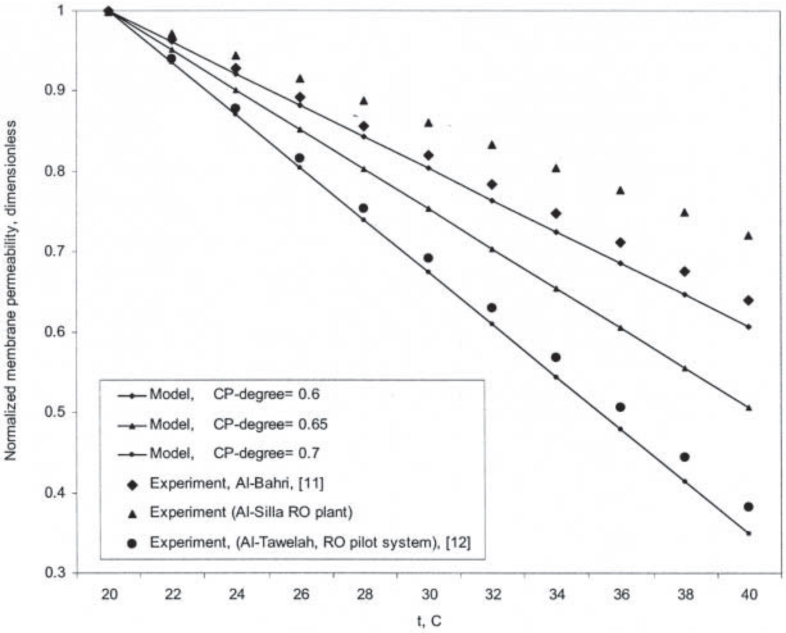

Figure 12. Normalized membrane permeability vs. operating temperature (Comparison of calculated projections with experimental results from[11] and.[12] Calculated projections correspond to $R_{M(apparent)} = 0.992$, (or $R_{M(true)} = 0.995$).

The calculated projections based on Eqs (17), (13), (1) and available experimental reference data are given in Fig. 12. The data on normalized permeability are represented in nondimensional form where the temperature ranges from 20 to 40°C. Correspondence between calculated projections and available empirical results are shown in Fig. 12. The behavior of calculated projections is strongly influenced by the CP degree. Lack of experimental data on surface concentration (or the CP degree) hampers quantifying the deviation between experimental and calculated results. Available experimental data can be used only for comparison of general trends of behavior.

7. CONCLUSIONS

The behavior of CP-resistance and normalized permeability against temperature is influenced by the surface concentration and CP degree that, in turn, is dependent upon transport characteristics of membranes such as the degree of membrane rejection.

The growth of surface concentration (and the CP degree) can change the type of functional behavior of normalized permeability against temperature, namely, (A) at low level of CP degree the growth of temperature causes growth of the normalized permeability, while (B) at high level of the CP degree, the system is characterized by opposite behavior: the normalized permeability decreases with growth of temperature.

In cases when cooling water from heat rejection section of MSF (with elevated temperature) is used as a feed water for RO, the preference should be given to membranes with moderate salt rejection rather then membrane with high salt rejection.

A proposed submodel can be incorporated into algorithm for calculation of longitudinal profile of the CP degree and for optimization of regime parameters against temperature.

8. SYMBOLS

$A_{mem}(t)$	Specific permeability of membrane, m^3/m^2-s-bar
a	Coefficients in Guzman–Andrade equation, Pa s
b	Coefficient in Guzman–Andrade equation, T
C	Concentration, mol/m^3, ppm
P	Pressure, bar
$R_{M(OBSERVED)}$	Observed degree of membrane rejection $R_{M(OBSERVED)} = (C_1 - C_2)/C_1$, dimensionless
$R_{M(TRUE)}$	True (or intrinsic), degree of membrane rejection $R_{M(TRUE)} = (C_{1M} - C_2)/C_{1M}$ dimensionless
$r_{mem}(t)$	Hydraulic resistance of membrane, $[m^2$-s-bar$]/m^3$
$r_{CP\text{-}layer}(t, c)$	Hydraulic resistance of CP layer, $[m^2$-s-bar$]/m^3$
$r_{gel}(t, c)$	Hydraulic resistance of gel layer, $[m^2$-s-bar$]/m^3$
V	Transmembrane or transverse velocity, m/s
α	Degree of concentration polarization, $\alpha = (C_{1M} - C_1)/C_1$ dimensionless
ρ	Density, kg/m^3
π	Osmotic pressure, bar
μ	Dynamic viscosity, Pa s

Subscripts

1	identifies parameter corresponding to the bulk of solution;
1M	identifies parameter corresponding to membrane surface;
2	identifies parameter corresponding permeate

Appendix A. Upper limit of the CP degree. (Influence of temperature and degree of membrane rejection on the upper limit of CP degree*.) Input data: $\Delta P = 70\,\text{bar}$, $C_1 = 45000\,\text{ppm}$ ($\sim 769\,\text{mol/m}^3$).

No	True degree of membrane rejection, dimensionless	Operating temperature, °C										
		20	22	24	26	28	30	32	34	36	38	40
1	R_M(true) = 0.1	17.69	17.56	17.44	17.31	17.19	17.07	16.95	16.83	16.72	16.61	16.49
2	R_M(true) = 0.2	8.34	8.28	8.22	8.16	8.10	8.04	7.98	7.92	7.86	7.80	7.75
3	R_M(true) = 0.3	5.23	5.19	5.15	5.10	5.06	5.02	4.98	4.94	4.91	4.87	4.83
4	R_M(true) = 0.4	3.67	3.64	3.61	3.58	3.55	3.52	3.49	3.46	3.43	3.40	3.37
5	R_M(true) = 0.5	2.74	2.71	2.69	2.66	2.64	2.61	2.59	2.57	2.54	2.52	2.50
6	R_M(true) = 0.6	2.11	2.09	2.07	2.05	2.03	2.01	1.99	1.97	1.95	1.93	1.92
7	R_M(true) = 0.7	1.67	1.65	1.63	1.62	1.60	1.58	1.56	1.55	1.53	1.52	1.50
8	R_M(true) = 0.8	1.34	1.32	1.30	1.29	1.27	1.26	1.24	1.23	1.21	1.20	1.19
9	R_M(true) = 0.9	1.08	1.06	1.05	1.03	1.02	1.01	0.99	0.98	0.97	0.96	0.94
10	R_M(true) = 1.0	0.87	0.86	0.84	0.83	0.82	0.81	0.80	0.78	0.77	0.76	0.76

*Calculated values are based on Eq. (26), where $\alpha_{\max}(t) = \Delta P[R_{M(TRUE)}(iC_1RT)]^{-1} - 1$

9. LITERATURE

1. Al-Marafie, M.R. Prospects of hybrid RO/MSF desalting plants in Kuwait. Desalination **1989**, *72*, 395–404.
2. Awerbuch, L. Power-desalination and importance of hybrid ideas. In *IDA World Congress on Desalination*; Spain, 6–9 Oct. 1997; Vol. 4, 184–192.
3. Kamaluddin, B.A.; Talavera, J.L.; Wangnik, K. Reverse osmosis seawater desalination systems in co generation plants for additional production of drinking water using off-peak electrical energy. In *IDA World Congress on Desalination*; Spain, 6–9 Oct. 1997; Vol. 1, 387–413.
4. Wangnik, K. A global overview of water desalination technology and the perspectives. In *Int. Conference Spanish Hydrological Plan and Sustainable Water Management. (Environmental Aspects, Water Reuse and Desalination)*; Zaragossa, Spain, 13–14 June 2001.
5. Mark, W.; Klinko, K. Optimization of seawater RO systems design. Desalination **2001**, *138*, 299–306.
6. Humphries, R.; Davies, K.; Ackert, J. Nuclear desalination using preheated feed water: an advanced RO system coupled with a CANDU nuclear reactor. In *IDA World Congress on Desalination and Water Reuse*; Manama, Bahrain, 8–13 March 2002.
7. Ho, W.S.; Sirkar, K. *Membrane Handbook*; Van Nostrand: New York, 1998.
8. Elimelech, M.; Bhattacharjee, S. A novel approach for modeling concentration polarization in crossflow membrane filtration based on the equivalence of osmotic pressure model and filtration theory. Journal of Membrane Science **1998**, *145*, 223–241.
9. Michael, J.H.; Snow, et al.; New technique for extreme conditions: high temperature reverse osmosis and nanofiltration. Desalination **1996**, *105*, 57–61.
10. Sergei, P. Agashichev; Khaled, N. Lootah. The influence of temperature and permeate recovery on energy consumption of a reverse osmosis system. Desalination **2003**, *154*, 253–266.
11. Al-Bahri, Z.K.; Hanbury, W.T.; Hodgkiess, T. Optimum feed temperature for seawater reverse osmosis plant operation in an MSF/SWRO hybrid plant. Desalination **2001**, *138*, 335–339.
12. Agashichev, S.; Rizk, M.; Shahzad, K.; Hisham, H.; El-Dahshan, M.E. *Evaluation of Reverse Osmosis Plant for Seawater Desalination, Report PWDRC-DL-001/2003*; ADWEA: Abu Dhabi, UAE, 2003.
13. Perry, R.H.; Green, D.W., Eds.; *Perry's Chemical Engineers' Handbook*, 7th Ed.; McGraw-Hill: New York, 1997.